Transport in a small Aspect Ratio Torus[*]

R.B. White, D.A. Gates & H.E. Mynick

Princeton Plasma Physics Laboratory, P.O. Box 451, Princeton, NJ, USA 08543-0451

Transport in a small Aspect Ratio Torus[1]

R.B. White, D.A. Gates & H.E. Mynick

Princeton Plasma Physics Laboratory, Princeton, NJ, 08543, USA

e-mail contact: rwhite@pppl.gov

Abstract. Transport theory in toroidal devices often assumes large aspect ratio and also assumes the poloidal field is small compared to the toroidal field. These assumptions result in transport which in the low collision rate limit is dominated by banana orbits, giving the largest collisionless excursion of a particle from an initial flux surface. However in a small aspect ratio device the gyro radius may be larger than the banana excursion, resulting in significant deviations from the standard neoclassical predictions. In this paper we report numerical simulation of diffusion in low and high beta low aspect ratio equilibria. We also sketch an analytic theory. The diffusion, which we refer to as omniclassical, is a combination of neoclassical and properly averaged classical effects, and can be two or three times the neoclassical value. Good agreement of the analytic theory with numerical simulations is obtained.

In tokamaks with low aspect ratio ("spherical tori") the transport rate predicted by a Lorentz (*ie*, full-orbit) code GYROXY [1] is substantially larger than the rate computed using guiding-center (GC) codes such as ORBIT. [2] The drift-kinetic equations used by GC codes are also the basis of standard neoclassical theory [3,4], so the disparity between the GC and Lorentz results indicates that something is missing in neoclassical theory, related to the effects of finite gyroradius for devices with low aspect ratio $A \equiv R/a$ (R and a are the device major and minor radii), and larger ratios B_p/B_t of the poloidal to toroidal magnetic field than those found in larger-A tokamaks. The total transport including these new effects has been termed [5] "omniclassical transport."
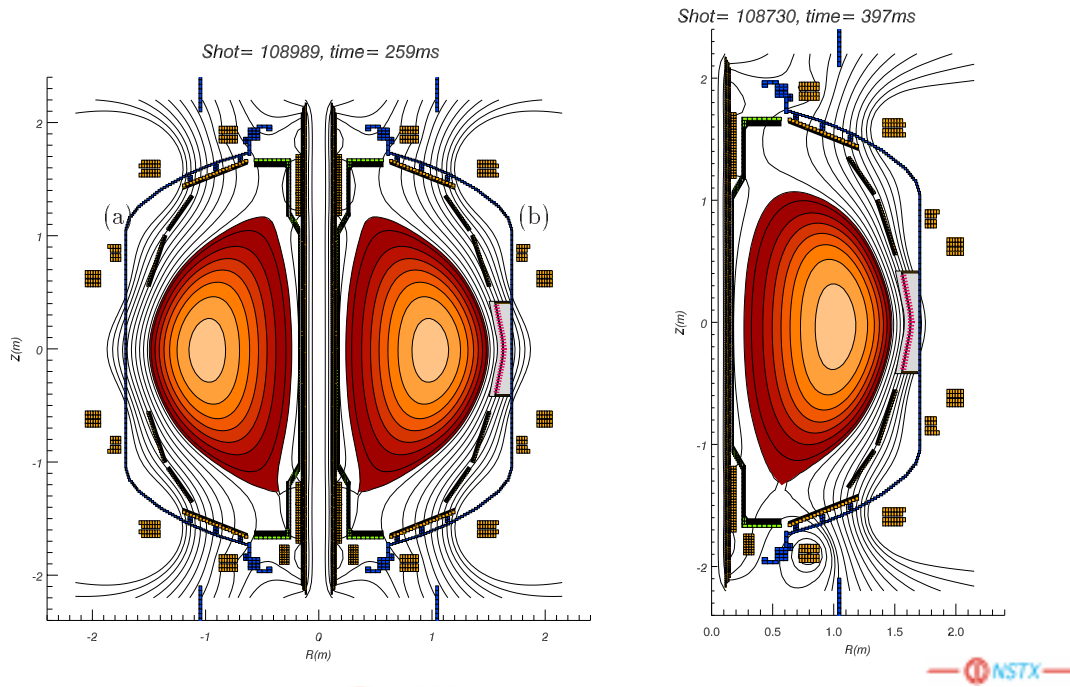
FIG. 1. The double null discharge has $B_\phi(0) = 0.3T$ $R = 0.86m$ and $I_p = 1.2MA$, $\beta_t = 35\%$. The single null discharge has $B_\phi(0) = 0.45T$ and $I_p = 0.8MA$, $\beta_t = 15\%$.

In this work, we report numerical simulations using the guiding center code ORBIT and the full Lorentz code GYROXY, and provide an explanation for the omniclassical enhancement over the neoclassical rates observed with the ORBIT code. The explanation is a generalization of the classical transport one expects in a 1-dimensional (1D) or large-A (weakly 2D) system, where the diffusion coefficient $D_{cl} \simeq \nu \rho_g^2$ is small compared with the neoclassical coefficient $D_{nc} \simeq \nu (q\rho_g)^2 / \epsilon^{3/2}$ (with ν the collision frequency, ρ_g the particle gyroradius, and $\epsilon \equiv A^{-1}$).

In the GC code, a collision operator $C = C_\parallel$ is used which scatters only in pitch $\lambda \equiv v_\parallel / v_\perp \equiv v \cos_v$, where v is the particle speed, and $v_\parallel$ and $v_\perp$ are its components parallel and perpendicular to the magnetic field $\mathbf{B}$. This permits the particle "banana center" (bounce-averaged flux surface label) $\bar{x}$ to wander diffusively. In GYROXY, as well as in the analytic calculation, C scatters not only in λ, but also in gyrophase ϕ_v, $C = C_\parallel + C_\perp$, providing a second statistically independent process by which $\bar{x}$ can wander, enhancing the overall transport. The analytic theory finds that the classical transport has two contributions, one from scattering in λ, and a dominant contribution from scattering in ϕ_v. When the collision operator in GYROXY is constrained to scatter only in λ, we find that the transport rate drops toward that from ORBIT by an amount consistent with the theory.

Figure 1 shows two equilibria [6] in the National Spherical Torus Experiment [7] (NSTX) spherical torus. The double null discharge is a high beta discharge, with a toroidal beta of 35 percent, with $B_\phi(0) = 0.3T$ $R = 0.86m$ and $I_p = 1.2MA$. The single null discharge has beta of 15 percent and $B_\phi(0) = 0.45T$ and $I_p = 0.8MA$. Figure 2 shows two banana orbits in the high beta NSTX equilibrium of Fig. 1 and a close up view of the banana near the outboard edge. The cyclotron excursion is much larger than the guiding center banana width, and thus we expect neoclassical results to give an underestimation of the transport. Note that the ratio of cyclotron width to banana width is independent of particle energy, *ie* this is a result of field geometry, not high particle energy, and is in fact energy independent.
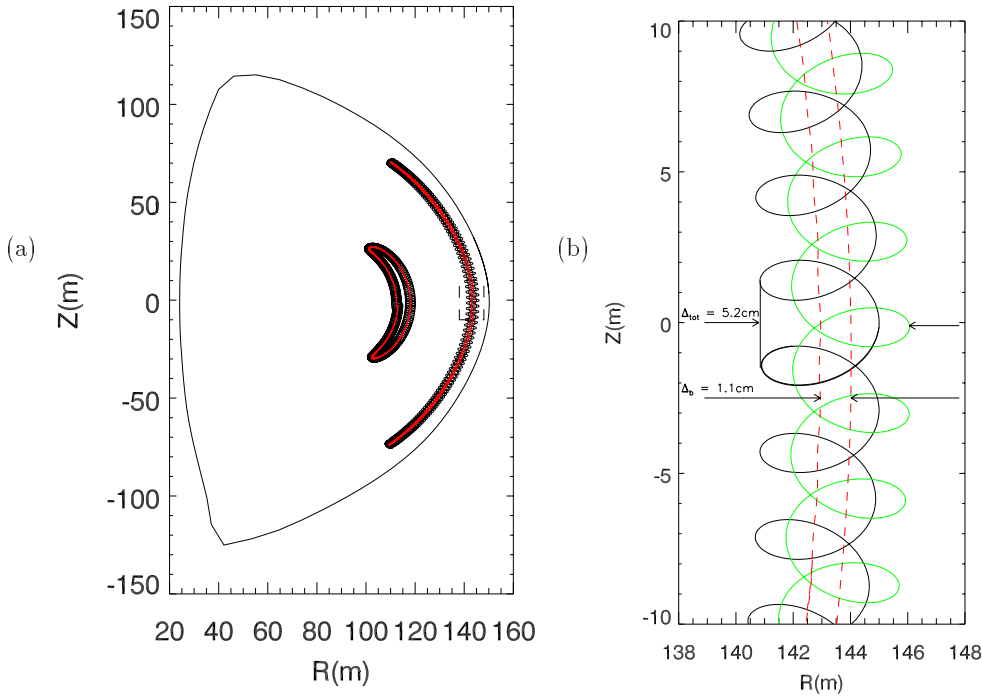
FIG. 2. In (a) are shown two banana orbits in NSTX. In (b) is shown a blowup of the midplane section of the banana orbit at larger minor radius. The black trace is the downward drifting part of the full orbit, Green is the upward drifting part. Red dashed line is the gyro averaged orbit. The excursion is much larger than the banana width.

The collision operator in the two representations is of course very different. In the guiding center code the pitch $\lambda = v_\parallel / v$ is changed each time step according to the Monte Carlo prescription [8]

$$\lambda' = \lambda(1 - \nu dt) \pm ((1 - \lambda^2)\nu dt)^{1/2} \tag{1}$$

where ν is the collision frequency, dt is the time step, and the plus or minus sign is chosen randomly. This produces a Gaussian spread of the particle pitch while conserving energy. In GYROXY the velocity vector is moved through an angle given by νdt on the surface of the sphere $\vec{v} = constant$. In Fig. 3 is shown a numerical confirmation of the equivalence of these two operators, acting on a large distribution of particles initially with pitch zero.
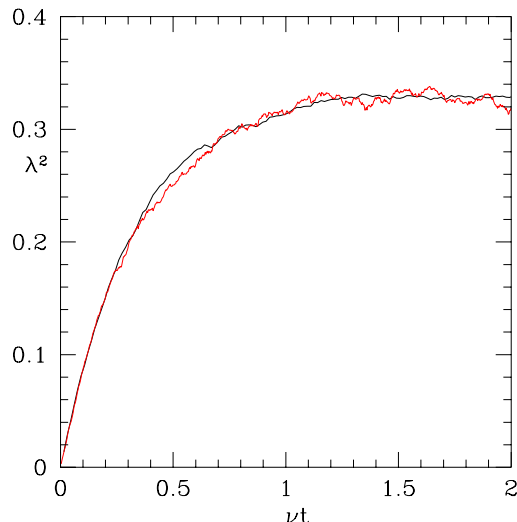
FIG. 3. Equivalence of the collision operators in the two representations. The black curve is from ORBIT and the red curve from GYROXY. A collection of particles initially with zero pitch is acted upon by the collision operator alone, with no motion in space, equilibrating in about one collision time. Shown is the mean squared pitch for the distribution as a function of time.

The simulations are performed by loading a monoenergetic distribution of particles on a surface ψ_0 (ψ is the poloidal flux$/2\pi$) uniformly in poloidal angle and pitch variable λ. Integrating the particle orbits, D is computed from the Fokker-Planck expression $D = (1/2)d/dt\langle(\delta\psi)^2\rangle(t)$.

In Fig. 4 we plot $\langle(\delta\psi)^2\rangle$ (arbitrary units) versus time from GYROXY and ORBIT, for a high beta equilibrium in the National Spherical Torus Experiment [7] (NSTX) spherical torus with a 100 eV monoenergetic distribution launched on a surface ψ with maximum major radius $X(\psi) = 140$ cm. The collision frequency used is $10^{-4}\omega_0$, with ω_0 the cyclotron frequency, which is well within the banana regime.

The top curve (a) is from GYROXY with full collision operator $C = C_\parallel + C_\perp$, the bottom curve (c) is from ORBIT, which has $C_\parallel$ only, and the middle curve (b) is from GYROXY with $C_\parallel$ only. One notes that the slope of this curve has dropped most of the way from that of the full-C GYROXY curve to the ORBIT curve, as indicated above. The rapid displacement from the flux surface occuring initially reflects the mean square banana width in the case of ORBIT, and the much larger banana plus gyro width for the upper two curves. We have also verified the irrelevance of the distribution in energy by reproducing the same results using a Maxwellian distribution.
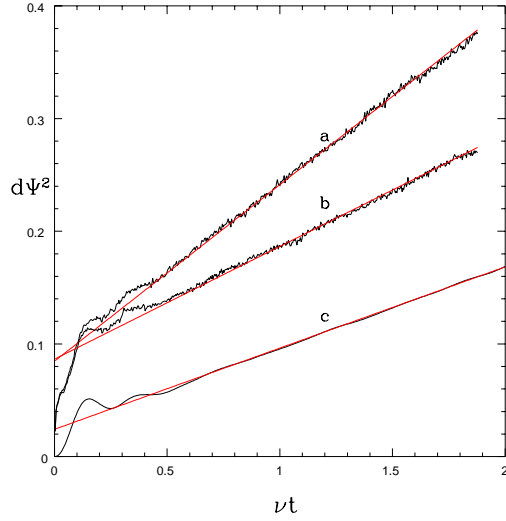
FIG. 4. Numerically observed spreading of initial particle distribution. Curve c shows the result using guiding center motion only. Curve b shows the result with pitch angle scattering only. The initial large excursion is due to the cyclotron excursions, and the slope of the long time motion gives the diffusion. Curve a is the result of full cyclotron motion and a complete collision operator.

In Fig. 5 we plot the numerically obtained D/D_{nc} versus $X(\psi)$ for the high beta equilibrium, where D_{nc} is the GC result from ORBIT. The top curve (a) gives results using the full collision operator C, and the bottom curve (b) with C constrained to $C_{\parallel}$ only. Doing so removes about 3/4 of the disparity between the GYROXY and ORBIT results.
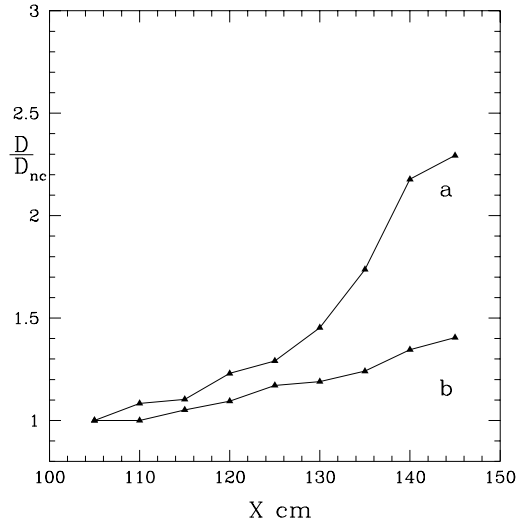
FIG. 5. Numerical diffusion rates, normalized to the neoclassical value, for the high beta equilibrium. Curve b shows the result of full cyclotron motion with pitch angle scattering only. Curve a is the result of full cyclotron motion and a complete collision operator

To gain an analytic understanding of these results, we consider the diffusion of particles in the space of the three constants of motion $\mathbf{J}$, and in particular, diffusion in the banana-center flux surface $\bar{x}$. (A typical choice for $\mathbf{J}$, employed in the "action-angle formalism" [9], are the magnetic moment J_g, the bounce action J_b, and the angular momentum p_ζ. For our limited purposes here, we shall only need to make use of a small part of the machinery of this formalism.) One may define $\bar{x}$ using the conservation of $p_\zeta \equiv \mathbf{e}_\zeta \cdot \mathbf{p} \equiv \frac{e}{c} A_\zeta + M v_\zeta$ for collisionless orbits. Here, $\mathbf{e}_\zeta = R\hat{\zeta}$ is the contravariant basis vector for toroidal azimuth ζ. We use a flux coordinate system $(x, , \zeta)$, with x the flux-surface label. The vector

potential is given by $\mathbf{A} = \Phi\nabla - \psi\nabla\zeta$, with $A(x) = \Phi$ the toroidal flux$/2\pi$, and $A_\zeta(x) = -\psi$. Thus, $p_\zeta = -\frac{e}{c}\psi + Mv_\zeta$, and for this reason, expressions are somewhat simpler if one adopts the choice $x \to \psi$, which we now do. Since p_ζ is a constant of the motion, it equals its orbit-average $\bar{p}_\zeta = \frac{e}{c}\bar{\psi} + M\bar{v}_\zeta$, and thus

$$\bar{\psi} = -\frac{c}{e}(p_\zeta - M\bar{v}_\zeta) = \psi - \frac{c}{e}M(v_\zeta - \bar{v}_\zeta). \tag{2}$$

After a little geometry, one can write v_ζ in terms of the more conventional components $v_\parallel, v_\perp$ as

$$v_\zeta = R(b_t v_\parallel + b_p v_\perp \cos\phi_v) = Rv(b_t\lambda + b_p\sqrt{1 - \lambda^2}cos\phi_v) \equiv v_{\zeta\parallel} + v_{\zeta\perp}, \tag{3}$$

where $b_{t,p} \equiv B_{t,p}/B$, the ratio of the toroidal or poloidal to the total magnetic field.

For trapped particles (trapping-state index $\tau = 0$), one has $\bar{v}_\zeta = 0$. For passing particles ($\tau = 1$), $\bar{v_{\zeta\perp}}$ again vanishes under the gyro-average, while $\bar{v_{\zeta\parallel}} \simeq v_{\zeta\parallel}$, an approximation improving for more deeply-passing particles. Thus, in Eq. 2, one has

$$(v_\zeta - \bar{v}_\zeta) \simeq (1 - \tau)v_{\zeta\parallel} + v_{\zeta\perp}. \tag{4}$$

As in the GYROXY simulations, we adopt a collision operator which scatters in λ and ϕ_v, but not in energy:

$$C \equiv C_\parallel + C_\perp \equiv (\nu v^2/2)\nabla_\mathbf{v} \cdot (\mathbf{I} - \hat{\mathbf{v}}\hat{\mathbf{v}}) \cdot \nabla_\mathbf{v} = \nu/2[\partial_\lambda(1 - \lambda^2)\partial_\lambda + (1 - \lambda^2)^{-1/2}\partial_{\phi_v}^2]. \tag{5}$$

$C_\parallel$ is the usual Lorentz collision operator used in the drift-kinetic framework. Both $C_\parallel, C_\perp$ are self-adjoint in (λ, ϕ_v) space: for any functions F, G,
$\int d^2\mathbf{v}FC_{\parallel,\perp}G = \int d^2\mathbf{v}GC_{\parallel,\perp}F$.

We compute the radial flux of banana centers due to the action of C:
$d_t\langle\bar{\psi}\rangle \equiv \langle C\bar{\psi}\rangle$, where d_t is the collisionally-induced time derivative, and for any function $F(z)$, $\langle F\rangle \equiv V^{-1}\int_V d^6zfF$ is a phase-space integral ($d^6z = d^3\mathbf{x}d^3\mathbf{p}$) of F weighted by distribution function f, over a thin toroidal shell of volume V centered at flux surface ψ. From Eq. 5, one has $d_t = d_t^\parallel + d_t^\perp$, yielding contributions to the flux induced by $C_\parallel$ and $C_\perp$, respectively. From Eqs.2-5, one thus has

$$d_t\langle\bar{\psi}\rangle = (-\frac{c}{e}M)d_t\langle(v_\zeta - \bar{v}_\zeta)\rangle = (-\frac{c}{e}M)\langle(C_\parallel + C_\perp)[(1 - \tau)v_{\zeta\parallel} + v_{\zeta\perp}]\rangle, \tag{6}$$

which one sees gives four terms, of which the term $\langle C_\perp(1 - \tau)v_{\zeta\parallel}\rangle$ vanishes. The first term is the neoclassical flux, $\Gamma_{nc} \equiv (-\frac{c}{e}M)\langle(C_\parallel(1 - \tau)v_{\zeta\parallel}\rangle$, while the remaining two yield the generalized classical flux, $\Gamma_{cl} \equiv (-\frac{c}{e}M)\langle(C_\parallel + C_\perp)v_{\zeta\perp}\rangle$.

To complete the calculation, we need an expression for the particle distribution f. Any function $f = f_0(\mathbf{J})$ of $\mathbf{J}$ satisfies the Vlasov equation, so for low ν, a good collisionless approximation is the local Maxwellian form $f_0(\bar{\psi}, E) = n_0/[2\pi TM]^{3/2}\exp(-E/T)$, with n_0 and T functions of $\bar{\psi}$, and $E \equiv Mv^2/2$ the particle energy. Using $\bar{\psi} = \psi - \delta\psi$, one has $f_0(\bar{\psi}) \simeq f_0(\psi) - \delta\psi\partial_\psi f_0$, where $\partial_\psi f_0 = -\kappa f_0$, with $\kappa = \kappa_n + \kappa_T(v^2/v_T^2 - 3)/2$, $\kappa_n \equiv -\partial_\psi\ln n_0$ and $\kappa_T \equiv -\partial_\psi\ln T$. From Eqs.2 and 4, $\delta\psi = (\frac{c}{e}M)((1 - \tau)v_{\zeta\parallel} + v_{\zeta\perp}) \equiv \delta\psi_b + \delta\psi_g$, with $\delta\psi_g$ the gyro-orbit radial excursion, and $\delta\psi_b$ the (bounce-related) radial drift excursion. Using these in Eq. 6, one finds

$$d_t\langle\bar{\psi}\rangle = -V^{-1}\int_V d^6z\partial_\psi f_0\frac{\nu}{2}(\frac{c}{e}MRv)^2 \times$$
$$\{(1 - \tau)b_t^2(1 - \lambda^2) + b_p^2[(1 - 2\lambda^2) + \sqrt{1 - \lambda^2}]\cos^2\phi_v\} \tag{7}$$

The integrations over λ and ϕ_v here are elementary, and those over and v may be done for specific models. Setting $\kappa_T = 0$ to extract only the diagonal term D^ψ of the transport matrix, we find from Eq. 7

$$d_t\langle\bar{\psi}\rangle = -\partial_\psi n_0[\bar{D}_{nc}^\psi(\psi) + \bar{D}_{cl}^\psi(\psi)] = \kappa_n V^{-1}\int_V d^6zf_0[D_{nc}^\psi(v, \mathbf{x}) + D_{cl}^\psi(v, \mathbf{x})], \tag{8}$$

where $D_{nc}^{\psi}(v, \mathbf{x}) = \frac{1}{2}\nu\rho_g^2(B_t R)^2(1 - B/B_\pi)^{1/2}$, and

$D_{cl}^{\psi}(v, \mathbf{x}) = \frac{1}{4}(\frac{1}{3} + \frac{\pi}{2})\nu\rho_g^2(B_p R)^2$ are the neoclassical and generalized classical diffusion coefficients, which must be integrated over and v to obtain the averaged coefficients. Here, $B_\pi \equiv B(\psi, = \pi)$ is the maximum value of B on surface ψ. The factor $\frac{1}{3}$ in D_{cl}^{ψ} is the contribution from the term $C_{\parallel}v_{\zeta\perp}$ in Eq. 6, which is a new term, not present in the classical scattering expressions. The dominant factor $\frac{\pi}{2}$ is from the term $C_{\perp}v_{\zeta\perp}$, which is the generalization of the usual "classical" contribution, with the appropriate factor $(B_p R)^2$ to be used in the flux surface average. Thus, removing $C_{\perp}$ from the GYROXY simulation should remove most of the enhancement of D over D_{nc}, as seen in Fig. 5. The dominant contribution from this approximate theory is about $\frac{\pi}{2}/(\frac{1}{3} + \frac{\pi}{2}) \simeq 82\%$ of D_{cl}, while the factor in Fig. 5 is about 70%. Note that ratios of these quantities are independent of particle energy, being due to equilibrium field geometry, and thus these results apply to heat transport as well as particle transport.

We put these diffusion coefficients in a more familiar form by transforming from ψ to a flux function $r(\psi)$ having units of length, which approximates an average minor radius. One has $d_t\langle \bar{r} \rangle = -\partial_r n_0 \bar{D}^r$, with $\bar{D}^r = (\partial_\psi r)^2 \bar{D}^\psi$, and similarly for D^r. Taking $r \equiv \sqrt{2\Phi/B_0}$, with B_0 the toroidal field strength on the magnetic axis, one has $(\partial_\psi r) = (q/B_0 r)$, and thus

$D_{nc}^r(v, \mathbf{x}) = \frac{1}{2}\nu(\rho_g q)^2(B_t R/B_0 r)^2(1 - B/B_\pi)^{1/2}$, and

$D_{cl}^r(v, \mathbf{x}) = \frac{1}{4}(\frac{1}{3} + \frac{\pi}{2})\nu\rho_g^2(qB_p R/B_0 r)^2$.

The θ-dependences in these expressions lie in $\rho_g, (1 - B/B_\pi)$, and $B_p R$. For a small-ϵ device, $\rho_g \simeq$ const, $\oint \frac{d}{2\pi}(1 - B/B_\pi)^{1/2} \simeq \frac{2}{\pi}\sqrt{2\epsilon}$, $(B_t R/B_0 r)^2 \simeq 1/\epsilon^2$, and $(qB_p R/B_0 r)^2 \simeq 1$, resulting in the familiar dependences

$D_{nc}^r(v, \mathbf{x}) \simeq \sigma_{nc}\nu(\rho_g q)^2/\epsilon^{3/2}$ and $D_{cl}^r(v, \mathbf{x}) \simeq \sigma_{cl}\nu\rho_g^2$, with numerical coefficients $\sigma_{nc} = \frac{\sqrt{2}}{\pi}$, and $\sigma_{cl} = \frac{1}{4}(\frac{1}{3} + \frac{\pi}{2})$.

(a)
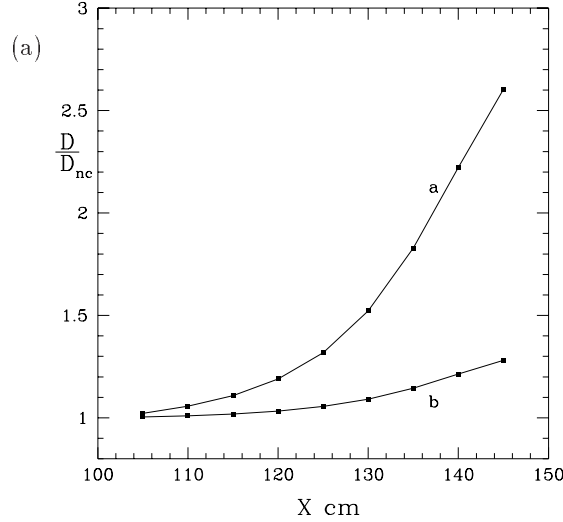
FIG. 6. Analytic diffusion rates, normalized to the neoclassical value, Curve b shows the result of full cyclotron motion with pitch angle scattering only. Curve a is the result of full cyclotron motion and a complete collision operator.

In Fig. 6 is shown the average of these expressions using the NSTX geometry to compute the analytic counterparts of the numerical results. One notes the approximate agreement of the numerical results in Fig. 5 and the analytic results.

Finally, to display the dependence on the equilibrium beta, in Fig. 7 are shown the numerical and analytic results using the full collision operator for both the low beta and the high beta NSTX equilibrium.
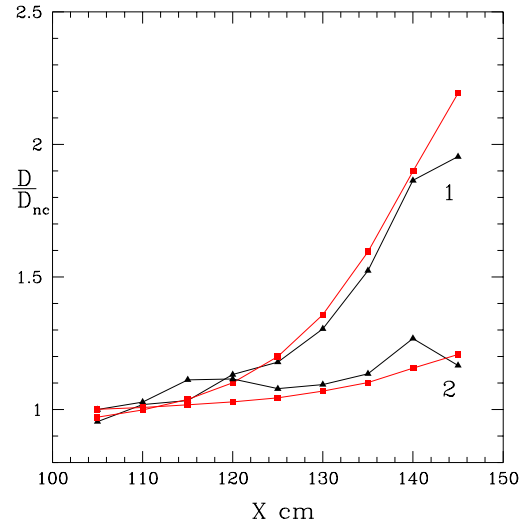
FIG. 7. Numerical (black triangles) and analytic (red squares) diffusion rates, normalized to the neoclassical value, for the high beta equilibrium (1), and the low beta equilibrium (2).

1. Summary

Summarizing, we have performed numerical simulations of diffusion using guiding center and full Lorentz codes, and provided an explanation for the omniclassical enhancement of the total transport over neoclassical rates. We developed an approximate transport theory which predicts the enhancement of the transport over neoclassical given by the full-orbit GYROXY code with full collision operator, and displays the two parts of the finite-gyroradius transport due to pitch angle scattering and gyro phase scattering. The enhancement comes from a generalization to strongly 2D geometries of classical transport, which for low-A configurations like NSTX can dominate over the neoclassical contribution. The dominant contribution of the cyclotron motion is from the gyro phase scattering, but there is also a sizeable contribution from pitch angle scattering. This result indicates that the use of neoclassical expressions to calculate particle and energy loss in devices such as NSTX can lead to significant underestimation of these processes.

[1] Liu Chen, Zhihong Lin, R.B. White, *Phys. Plasmas* **8** 4713 (2001)

[2] R.B. White, M.S. Chance,*Phys. Fluids* **27**, 2455 (1984).

[3] F.L. Hinton, R.D. Hazeltine, *Rev. Mod. Phys* **48**, Part 1, 239 (1976).

[4] C.S. Chang, F.L. Hinton, *Phys. Fluids* **25**, 1493 (1982).

[5] D.A. Gates, H. Mynick, R.B. White *Phys. Plasmas***11** L45 (2004).

[6] D. A. Gates and the NSTX nationsl research team *Phys. Plasmas***10** 1659 (2003)

[7] M. Ono *et al*, *Nucl Fusion* **40**, 557 (2000).

[8] A. Boozer and Kuo-Petravick *Phys. Fluids***24** 851 (1981).

[9] A. N. Kaufman, *Phys. Fluids* **15**, 1063 (1972).